Exploring Methods for Optic Disc and Optic Cup Segmentation: A Review for Glaucoma Diagnosis

Eslam Elsheikh
School of Information Technology and Computer Science, Nile University
Giza, Egypt
es.elsheikh@nu.edu.eg

Mustafa Elattar
Medical Imaging and Image Processing Research Group, Center for Informatics Science, Nile University, School of Information Technology and Computer Science, Nile University, Giza, Egypt
MElattar@nu.edu.eg

***Abstract*—Glaucoma is an eye condition that can damage the optic nerve and may lead to loss of vision if not diagnosed and treated timely [1], Glaucoma can affect people of all ages but its most common in adults over 40 [2], Glaucoma is considered second leading cause of blindness in the world [3], Glaucoma diagnostic is not an easy and it needs careful optic nerve evaluation before deciding treatment, there is commonly five factors should be checked to exam an eye for glaucoma (1) the inner eye pressure "Tonometry", (2) the shape and color of the optic nerve "Ophthalmoscopy", (3) the complete field of vision "perimetry", (4) the angle in the eye where the iris meets the cornea "Gonioscopy", (5) thickness of the cornea "Pachymetry" [3], ophthalmologists perform ophthalmoscopy using fundus camera views the eye's interior through the pupil, which is a small hole [4], our target in this paper is to provide literature review for different approaches used to analyze fundus images to detect glaucoma based on optic disc and optic cup segmentation.**

Keywords—Glaucoma, Optic Disc, Optic Cup, Retina, Fundus, Classification.

I. INTRODUCTION

Human eye is a complex organ, it has three layers "outer, middle and inner" the cornea and sclera together make the outer layer, the cornea function is to refract and transmits the light to the lens and retina, while sclera forms a connective tissue coat that protects the eye internal and external forces helping to maintain its shape, the middle layer is composed of the iris, ciliary body and choroid, while inner layer is the retina which is a complex layered structure of neurons that capture and process light [5], optic nerve contains of more than 1 million nerve fibers and it transmit the vision sensory information in the form of electrical pulses from the eye to brain, any damage to optical nerve can cause loss of vision [6], the optic nerve head also known as optic disc is the point where the axons from retinal ganglion cells leave the eye [7], figure 1 shows the optic nerve head (ONH)[8], figure 2 shows fundus image of an eye [5] Glaucoma is an eye condition that can damage the optic nerve and may lead to loss of vision if not diagnosed and treated timely, Glaucoma is one of the main causes of blindness in the world, Glaucoma diagnose is very challenging as symptoms usually appear at late stage, Glaucoma treatment is also challenging as the lost vision is irreversible due to loss of retinal neurons.

The most famous glaucoma indication is optic nerve head cupping and visual field loss and both symptoms are now considered the golden standard for glaucoma diagnosis [9]. WHO statistics show that by 2040 it is estimated that 111.8 million individuals will have glaucoma, studies show that 90% of those having glaucoma in some developed countries are undetected. glaucoma occurs anyway because of the inability of the eye to handle mechanical stress where the nerve fibers leave the eye or because of poor blood supply to these same nerve fibers. In glaucoma, the optic nerve gets damaged. A portion of the optic nerve may be assessed during the eye exam, where it can be seen as a round structure (optic disc), with the pink or reddish section representing the neural tissue that takes the visual information to the brain. The whitish central part represents absence of neural tissue, and it is called the "cup". Some amount of cupping is normal, but excessive cupping, or an increase in the amount of cupping over time, suggests glaucoma. There are many blood vessels that emerge from the optic disc to the retina. Glaucoma causes loss of the neural reddish tissue and there is progressive cupping of the optic disc – enlargement of the whitish central part [10]. Figure 3 (a, b, c) shows the difference between normal Optic Disc, Glaucomatous Optic Disc, and severe end-stage Glaucomatous Optic Disc.

In this survey paper the different techniques used to localize and perform segmentation for Optic Disc and Optic cup to detect glaucoma in fundus camera images based on Cup to Disc ratio factor is reviewed.

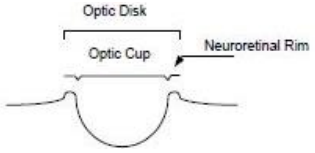

Fig. 1. Cross-section of The Optic Nerve Head

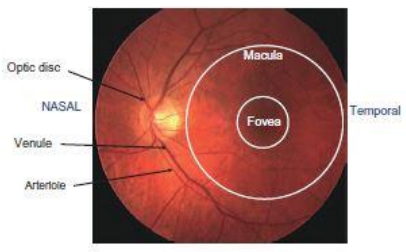

Fig. 2. Fundus of and eye

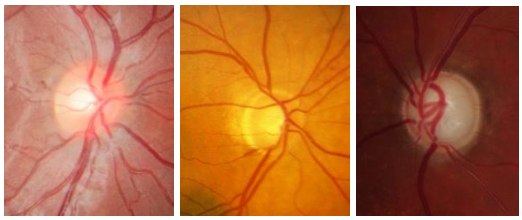

(a.) (b.) (c.)

Fig. 3. (a.) Normal Appearing Optic Disc: A normal optic disc shows a healthy and thick appearance of the neural tissue (reddish part), associated with a small cup (whitish central part), (b.) Glaucomatous appearing optic disc: Loss of the neural reddish tissue and increase of the optic disc cupping - enlargement of the whitish central part. There is a hemorrhage at the optic disc margin – which is usually related to uncontrolled glaucomatous disease, (c.) End-stage Glaucomatous Optic Disc: In end-stage glaucoma, there is almost no more neural tissue and eventually total cupping of the disc can be observed.

II. Literature Survey

Glaucoma detection and Optic Disc, Optic Cup segmentation techniques in this review are categorized to two main categories Classical techniques and Machine Learning techniques,

A. Classical Techniques:

Classical techniques are classified to three categories:

First, In Threshold based approach, Issac et al., 2015, [11] used completely adaptive and threshold-based technique using features from the image to perform optic disc and optic cup segmentation, while Nugraha & Soesanti, 2016, [12] used RED component of fundus image to apply contrast stretching followed by adaptive threshold, then morphological operation used to remove blood vessel. This resulted in more accurate calculation of optic disc and optic cup widths. Issac et al., 2015, technique was tested on local hospital images dataset of 63 images where ground truth was marked by hospital ophthalmologists for accuracy comparison, the model achieved optical disc and cup segmentation accuracy 92.06% on local hospital images, while Nugraha & Soesanti, 2016, technique applied on DRISTHIGS and RIM-ONE datasets, result of CDR is compared with ground truth.

Second, In Region based approach, Singh et al., 2014, [13] used automatic seed selection-based region growing technique to perform automated optic disc segmentation, this technique considered the center of optic disc a seed to apply the region growing, detection of optic disc center was automatically done by double windowing technique, moreover Omid et al., 2015, [14] introduced optic disc segmentation based on region growing technique after processing the fundus images using image thresholding based on entropy of input images histogram and binary morphological operations to find the seed point for region growing algorithm, applied average filtering technique for smoothing the images before applying region growing, and Salih et al., 2018, [15] automated optic disc segmentation based on seed localization using fast Fourier transform based template matching which obtains the seed on the optic disc to be used as input to the region growing stage to perform the segmentation of optic disc. Results of Singh et al., 2014, technique was compared to ground truth segmentation by ophthalmologists and accuracy was convincing with average computational time between 16 to 20 seconds, While Omid et al., 2015, [14] technique was applied to dataset of Shahid Labbafi Nedjad imaging center of Iran which has 120 high resolution fundus images of eye retina, the average sensitivity and specifity was 98.6%, 97.2% respectively, This algorithm achieved average segmentation computational time of 3.015 seconds, which was better computational time compared to Singh et al., 2014 technique, Moreover Salih et al., 2018, method achieved higher segmentation results compared to other known techniques based on DRIVE dataset as reference in terms of overlap, sensitivity, specificity, positive predictive value, accuracy, and kappa coefficient respectively of 87.16%, 91.27%, 99.81%, 90.56%, 98.68%, and 89.71%, computational wise this method achieved 1.03 seconds.

Third, In Clustering and Superpixel segmentation approach, Yin et al., 2012, [16] Used circular hough transform and statistical deformable model along with Blood vessel removal to automate Optic Disc and Optic Cup segmentation, While Cheng et al., 2013, [17] Used superpixel classification for initialization od Optic Disc boundary and deformable model is used to fine tune the Optic Disc boundary, moreover applied superpixel classification for detecting Glaucoma by computing Cup to Disc ratio (CDR) and perform Optic Disc and Optic Cup segmentation after computing center surround statistics from superpixels, and unify surround statistics from superpixels with histograms for Disc and Cup segmentation, Furthermore Ayub et al., 2016, [18] applied intensity weighted centroid method to get the region of Interest followed by preprocessing step then applied K-means clustering algorithm for Optic Disc and Optic cup segmentation finally ellipse fitting for boundary smoothening of Optic Disc and Optic Cup is applied, this technique is used to automatically compute CDR and detect Glaucoma from fundus images, Also Mohamed et al., 2019, [19] came up with glaucoma detection algorithm based on superpixel classification depending on multi phases technique. First anisotropic diffusion filter applied to input images as preprocessing phase to remove noise followed by illumination correction, preprocessing is then followed by pixel aggregation by applying superpixels using Simple Linear Iterative Clustering (SLIC) approach on input images, after pixels are aggregated features are extracted based on histogram data and textural information on each superpixel using statistical pixel-level (SPL) method, then extracted features are fed to Support Vector Machine (SVM) classifier to classify each superpixel into one of four classes (optic disc, optic cup, blood vessel, and background regions), this classifier is also used to determine the boundaries of both optic disc and optic cup, Finally, Segmented Optic Disc and Optic Cup are used to compute cup to disc ratio to detect Glaucoma, Moreover Rehman et al., 2019, [20] applied 3 phase preprocessing stage on fundus images including noise removal, image enhancement and image cropping, where

noise removal and image enhancement done using bilateral filtering followed by Optic Disc Localization and cropping region of interest (ROI) by using the green channel of fundus image which was used to find the most intense and least eccentric region to define Optic Disc centroid and crop ROI, followed by segmentation phase by applying superpixel SLIC technique then feature extraction as preparation step before training the classification models (SVM, RF Classifier, AdaBoost, Random under sampling) then applying ellipse fitting on segmentation result to estimate the optic disc edge region and eliminate the impact of noise introduced by vessels, Yin et al., 2012 method was tested on 325 fundus images with 0.92 Dice coefficient for Optic Disc segmentation and 0.81 for Optic Cup segmentation, while CDR Mean Absolute Error (MAE) was 0.1, as for Cheng et al., 2013 Cheng et al., 2013 technique was evaluated on 650 images with optic disc and optic cup boundaries manually marked by trained professionals, this technique show average overlapping error of 9.5% and 24.1% for optic disc and optic cup respectively, Ayub et al., 2016 method applied on 100 fundus images annotated by ophthalmologists and collected from Armed forces institute of ophthalmology (AFIO) Rawalpindi Pakistan divided to 73 normal images and 27 Glaucomatous images , Glaucoma detection accuracy reached 92% and CDR Mean Square Error (MSE) of 0.002, however Mohamed et al., 2019 proposed method tested on RIM-One dataset and successfully distinguished optic disc and optic cup from the background with an average accuracy and sensitivity of 98.6% and 92.3% respectively when using linear kernel, result of Rehman et al., 2019 method shows high accuracy of 99.3%, 98.8% and 99.3% respectively when applied on DRIONS, MESSIDOR and ONHSD databases,

B. Machine Learning Techniques:

Machine Learning techniques are classified to two categories:

First, In Hand crafted approach, Rao et al., 2015, [21] analyzed structural and energy features to classify Glaucomatous images, extracted and applied energy features to multi-layer perceptron (MLP) and back propagation (BP) neural network for effective classification by considering normal subject's extracted energy features, while Ruengkitpinyo et al., 2015, [22] used support vector machine (SVM) binary classifier to automatically detect glaucoma from retinal images of fundus camera, after applying optic disc and optic cup segmentation and feature selection to compute the cup to disc ratio (CDR) and rim width measurement to compute the ISNT rule, Moreover Dey & Bandyopadhyay, 2016, [23] applied principal component analysis (PCA) feature selection algorithm on fundus images after preprocessing images and performing noise removal and contrast enhancement techniques and finally performed classification by applying support vector machines (SVM) algorithm with linear kernel to classify fundus image as Glaucoma or Non Glaucoma, Finally Cheng et al., 2017, [24] proposed quadratic divergence regularized support vector machine (QDSVM) to perform transfer learning from domain with more training data to domains with lack of training data and different feature distribution, this overcomes the model generalization issue of retinal images which are usually collected in different conditions therefore a good performing model trained on one dataset may not perform well on another dataset, Thangaraj & Natarajan, 2017, [25] Built Non-Linear Support Vector Machine (SVM) model to perform Glaucoma classification task, Model was trained on labeled retinal images, proposed model have a five stage preprocessing step including image normalization in range [0,1], resize, RGB to Grey scale, applying 2D gaussian filter for noise removal and finally contrast improvement, later on preprocessed images pass through feature extraction step using Principal Component Analysis (PCA), from results perspective MLP-BP Artificial Neural Network (ANN) algorithm introduced by Rao et al., 2015 classifies the images in the database with the accuracy of 90.6%, while Dey & Bandyopadhyay, 2016 method achieved 96% Glaucoma classification accuracy, Cheng et al., 2017 show that after using transfer learning the classification error in superpixel level was reduced from 14.2% to 2.4%, moreover Thangaraj & Natarajan, 2017 model was tested on different datasets by taking subsample of each dataset including (DRIONS DB, RIM ONE and STARK PROJECT) and achieved 93% training accuracy using proposed technique.

Second, In Deep Learning approach, Abdullah et al., 2016, [26] used circular Hough transform and grow-cut algorithm for OD and OC localization and segmentation of Retinal Image Datasets on DRIVE, DIARETDB1, CHASE_DB1, DRIONS-DB, Messidor and one local Shifa Hospital Databases, When applied this methodology it achieved an optic disc detection success rate of 100% in DRIVE, DIARETDB1, CHASE_DB1, ONHSD and Shifa, However when applied on DRIONS-DB the OD detection decreased to 99.09%, Moreover The optic disc Segmentation based on this methodology achieved overlap ratio of 78.6%, 85.1%, 83.2%, 80.1%, 85.1%, 87.93%, and 86.1% in DRIVE, DIARETDB1, CHASE_DB1, Shifa, DRIONS-DB1, Messidor, and ONHSD databases, respectively, Moreover Sedai et al., 2016, [27] presented the cascade regression framework based on layer wise training of regressors to directly regress multidimensional optic cup and disc shape landmarks from image appearance, the methodology was applied to DRISHTI dataset and achieved an F-score of 0.95 ± 0.02 and 0.85 ± 0.08 for OD and OC segmentation respectively, Later on Sevastopolsky, 2017, [28] introduced modification of U-Net Convolutional Neural Network for Optic Disc and Cup Segmentation for Glaucoma Detection, Technique was tested on DRIONS-DB, RIM-ONE v.3, DRISHTI-GS, and achieved 0.89 OD segmentation IoU and dice score of 0.94 for DRIONS-DB, OD segmentation IoU of 0.89, Dice score of 0.95 and OC segmentation IoU of 0.69, Dice score of 0.82 when applied on RIM-ONE v.3, however when applied on DRISHTI-GS it achieved OC segmentation IOU of 0.75 and Dice score of 0.85, Further more Shankaranarayana et al., 2017, [29] came up with an improved architecture build upon Fully Connected Networks (FCNs) using the concept of residual learning called ResU-Net, Shankaranarayana et al., 2017 used fully convolutional and adversarial networks which was able to learn the mapping between retinal images and segmentation maps corresponding to it, this technique was applied on RIM-ONE dataset of 159 retinal images and achieved good results for Joint segmentation F-Score and IOU evaluation metrics, Joint segmentation F-Score and IOU was 0.977 and 0.901 respectively for OD segmentation and 0.945 and 0.786 respectively for OC segmentation, besides Xu et al., 2017, [30] proposed technique for optic disc localization based on Convolutional Neural Network (CNN) Architecture which are trained to find OD region suspected pixels, then candidate pixels are sorted out by threshold and center of

gravity of these pixels is calculated to find the OD location, proposed technique was then tested on multiple databases including ORIGA, MESSIDOR and STARE, while results was competitive compared to other localization techniques with localization accuracy of 100%, 99.43% and 89% for ORIGA, MESSIDOR and STARE respectively, and an average computation time of 0.93 s for STARE and 0.51s for Messidor,

Later on Fu et al., 2018, [31] used Deep learning M-Net architecture with polar transformation for the Fundus images to perform Joint OD and OC segmentation, then used the results of segmentation to compute CDR to detect Glaucoma, when this method was applied on ORIGA dataset it achieved average overlapping error 0.07 for OD segmentation and 0.23 for OC segmentation, this method also achieved an AUC of 0.85 and 0.9 for ORIGA and SCES datasets respectively, also Al-Bander et al., 2018, [32] Performed OD and OC segmentation based on deep learning DenseNet inherited by Fully Convolutional Network (FCN), during training phase ORIGA dataset was used then model was evaluated on multiple publicly available dataset of colour retinal fundus camera images without need to perform retraining on the datasets, datasets used for evaluation are DRIONS-DB, Drishti-GS, ONHSD and RIM-ONE, results for training and testing model on ORIGA dataset are 0.8723, 0.7788, 0.9986, 0.8768, and 0.9994 Dice score (F-measurement), Jaccard score (overlap), accuracy, sensitivity, and specificity for OD segmentation and 0.964, 0.9311, 0.9989, 0.9696, and 0.9994 for OC segmentation, moreover Jiang et al., 2018, [33] proposed a techniques using Faster RCNN which remove the Blood vessels and perform OD and OC object detection instead of segmentation and result bounding box for detected OD and OC and then internal tangential ellipses of these bounding boxes are the outputs as the segmentation results of optic disc and cup, this technique was applied on ORIGA data set and achieved average overlapping error of 6.9% and 22.2% for optic disc and cup segmentation, respectively, Later on Wang et al., 2019, [34] came up with patch-based Output Space Adversarial Learning framework (pOSAL) to segment the OD and OC jointly from different fundus image datasets "Drishti-GS, RIM-ONE-r3, REFUGE" Dice Index was used as performance matric for OD and OC segmentation respectively and resulted OD, OC dice index 0.965, 0.858 for Drishti-GS, 0.865, 0.787 for RIM-ONE-r3 and 0.9602, 0.8826 for REFUGE, furthermore Yu et al., 2019, [35] used modified version of U-Net architecture to perform OD and OC segmentation, the architecture combines pre-trained ResNet-34 model as encoding layers with classical U-Net decoding layers, the model trained on RIGA dataset and achieved an average dice value of 97.31% for disc segmentation and 87.61% for cup segmentation, later model fine tuning was done using Drishti-GS and RIM-ONE datasets, tuned model achieved average OD dice coefficient value of 97.38% and OC dice coefficient value of 88.77% for DRISHTI-GS test set, while RIM-ONE achieved OD dice coefficient of 96.10% and OC dice coefficient of 84.45% for RIM-ONE database, and Jiang et al., 2019, [36] used Joint RCNN model which is end-to-end region-based convolutional neural network for jointly segmentation of OD and OC, model trained and tested on ORIGA dataset and used overlapping error as evaluation matrix that achieved overlapping error of 6.3% for OC segmentation and 20.9% for OC segmentation, while CDR error was 6.8%, also Xu et al., 2019, [37] presented U-shaped CNN with multi-scale and multi-kernel module (MSMKU) for OD and OC segmentation, technique was validated on RIM-ONE-V3 and DRISHTI-GS datasets, evaluation metrices used were F-Score, IoU, sensitivity and specificity, for RIM-ONE-V3 OD segmentation F1-Score was 0.9561, IoU, sensitivity and specificity was 0.9172, 0.9521, 0.9987 for OD segmentation, while OC segmentation results on RIM-ONE-V3 dataset was 0.8564, 0.7586, 0.8515, 0.9971 for F-Score, IoU, sensitivity and specificity respectively, however DRISHTI-GS achieved better results compared to RIM-ONE-V3, were OD segmentation F1-Score was 0.9780, IoU, sensitivity and specificity was 0.9496, 0.9792, 0.9994, while OC segmentation results for DRISHTI-GS was 0.8921, 0.8232, 0.9157, 0.9989 for F-Score, IoU, sensitivity and specificity respectively,

In addition Sreng et al., 2020, [38] performed OD segmentation along with Glaucoma classification from fundus images by introducing deep learning model based on ensemble learning, ensemble technique performance was tested on RIM-ONE, ORIGA, DRISHTI-GS1 and ACRIMA datasets, it achieved best accuracy 99.53% with ACRIMA while DRISHTI-GS1 had worst accuracy 86.84 compared with other datasets used, as for RIM-ONE and ORIGA achieved accuracy of 97.37%, 90.00% respectively, moreover Area Under Curve (AUC) was also used as evaluation matrix, where RIM-ONE achieved 100% AUC, while ACRIMA achieved 99.98% AUC, however ORIGA and DRISHTI-GS1 had AUC 92.06%, 91.67% respectively, this method faced difficulties when tried to generalize on different datasets due to different ways other datasets are captured with different labelling criteria and different images quality, While Gao et al., 2020, [39] built an Recurrent Fully Convolution Network (RFC-Net) to automatically perform joint segmentation for OD and OC, model was evaluated on DRISHTI-GS1 and achieved F1-Score of 0.9787, 0.9058 for OD and OC segmentation respectively, proposed model was not tested to generalize tasks other that OD and OC segmentation from fundus images, moreover Tabassum et al., 2020, [40] built a Cup Disc Encoder Decoder Network (CDED-Net), this architecture can perform OD and OC segmentation jointly, where OD and OC are modeled as semantic pixel-wise labeling problem, proposed architecture was evaluated on DRISHTI-GS1, RIM-ONE, REFUGE datasets, evaluation took DC(F), JC(O), Sensitivity, Specificity as evaluation metrices, where DRISHTI-GS1 achieved DC(F), JC(O), Sensitivity, Specificity of 95.97%, 91.83%, 97.54%, 99.73% respectively for OD segmentation and 92.4, 86.32, 95.67, 99.81% for OC segmentation, while RIM-ONE resulted DC(F), JC(O), Sensitivity, Specificity of 95.82%, 91.01%, 97.34%, 99.73% respectively for OD segmentation and 86.22%, 75.32%, 95.17%, 99.81% respectively for OC segmentation, finally when tested on REFUGE the OD IoU was 0.8837, while OC IoU was 0.811 and MIoU was 0.8705,

III. Conclusion

This Survey paper presented different techniques and methods used to perform Optic Disc and Optic Cup segmentation to detect Glaucoma based on Cup to Disc Ratio (CDR), Presented techniques were categorized based on different used algorithms and Machine Learning techniques to achieve OD and OC segmentation, further supported by the detailed data presented in Tables 1, 2, and 3, which

respectively outline the availability of retinal image datasets, provide a comparative analysis of dataset characteristics, and highlight the distinctions between available segmentation and localization techniques.

Table 1. retinal images dataset public availability

Dataset	Public Availability	
	N	Y
RIM-ONE		11
ORIGA		6
DRIONS-DB		5
STARE		3
RIGA		2
REFUGE		2
CHASE_DB1		1
DIARETDB1		1
ACRIMA		1
Mettapracharak (Watraikhing) hospital	1	
local hospital images dataset	5	
SiMES	2	
ONHSD	2	
MESSIDOR	5	
DRIVE	4	
SCES	3	
ORIGA"light"	1	
DRISHTI-GS1	10	
Private Dataset from Armed Forces institute of ophthalmology (AFIO) Rawalpindi Pakistan	1	
Total publications (availability category)	34	32

Table 2. Dataset Detailed Comparative Analysis of Retinal Image Datasets

Dataset	Name	Dataset Link	Public (Y/N)	Total image Count	Normal	Pathology	Resolution (Pixels)	Format	Pathology (Y/N)	Labelling (Segmentation)	Annotation	Concinces (Y/N)	Notes	Reference
ACRIMA	ACRIMA	https://figshare.com/s/c2d31f850af14c5b5232	Y	705	309	396	2048 X 1536	JPEG	Y	Y	N	Y	Classification labels of normal and glaucomatous	Diaz-Pinto, A.; Morales, S.; Naranjo, V.; Köhler, T.; Mossi, J.M.; Navea, A. CNNs for automatic glaucoma assessment using fundus images: An extensive validation. Biomed. Eng. Online 2019, 18, 29. [CrossRef][PubMed]
CHASE_DB1	CHASE_DB1	https://blogs.kingston.ac.uk/retinal/chasedb1/	Y	28	NA	NA	1280 X 960	JPEG	NA	N	Y	NA	NA	NA
DIARETDB1	diabetic retinopathy database	http://www.it.lut.fi/project/imageret/	Y	89	5	84	1500 X 1152	PNG	Y	N	Y	Y	NA	NA
DRIONS-DB	Digital Retinal Images for Optic Nerve Segmentation Database	http://www.ia.uned.es/~ejcarmona/DRIONS-DB.html	Y	110	60	50	600 X 400	JPEG	Y	N	Y	Y	NA	NA
DRISHTI-GS1	DRISHTI-GS	https://cvit.iiit.ac.in/projects/mip/drishti-gs/mip-dataset2/Home.php	N "upon registration"	101	31	70	2896 X 1944	PNG	Y	NA	Y	Y	Manual segmentation masks of optic nerve head for 50 training images Classification labels of normal and glaucomatous	Sivaswamy, J.; Krishnadas, S.R.; Joshi, G.D.; Jain, M.; Tabish, A.U.S. Drishti-gs: Retinal image dataset for optic nerve head (onh) segmentation. In Proceedings of the 2014 IEEE 11th International Symposium on Biomedical Imaging (ISBI), Beijing, China, 29 April–2 May 2014; pp. 53–56. [CrossRef]
DRIVE	DRIVE: Digital Retinal Images for Vessel Extraction	http://www.isi.uu.nl/Research/Databases/DRIVE/	N	40	33	7	584 X 565	JPEG	Y	NA	NA	NA	NA	NA
MESSIDOR	Methods to Evaluate Segmentation and	http://www.adcis.net/en/third-party/messidor/	N "upon form approval"	1200	NA	NA	1440 X 960, 2240 X 1488,	TIFF	Y	Y	N	Y	NA	NA

	Indexing Techniques in the field of Retinal Ophthalmology						2304 X 1536								
ORIGA	Online Retinal Fundus Image Database for Glaucoma Analysis	NA	Y	650	482	16 8	3072 X 2048	JPE G	Y	Y	Y	Y	Segmentation masks of OD and OC Classification labels of normal and glaucomatous	Zhang, Z.; Yin, F.S.; Liu, J.;Wong,W.K.; Tan, N.M.; Lee, B.H.; Cheng, J.;Wong, T.Y. Origa-light: An online retinal fundus image database for glaucoma analysis and research. In Proceedings of the 2010 Annual International Conference of the IEEE Engineering in Medicine and Biology, Buenos Aires, Argentina, 31 August–4 September 2010; pp. 3065–3068.
ORIGA"light"	ORIGA-light	NA	N	650	482	16 8	NA	NA	NA	N	Y	NA	650 retinal images annotated by trained professionals from Singapore Eye Research Institute	Z. Zhang et al., "ORIGA-light: An online retinal fundus image database for glaucoma analysis and research," 2010 Annual International Conference of the IEEE Engineering in Medicine and Biology, 2010, pp. 3065-3068, doi: 10.1109/IEMBS.2010.5626137.
Private Dataset from Armed Forces institute of ophthalmology (AFIO) Rawalpindi Pakistan	AFIO	NA	N	100	73	27	NA	NA	NA	N	Y	Y	NA	NA

REFUGE	Retinal Fundus Glaucoma Challenge Edition	Ver 2 "restricted" : https://refuge.grand-challenge.org/Program2020/ Ver 1 "public": http://ai.baidu.com/broad/download?dataset=gon	Y	1200	1080	120	2124 X 2056	JPEG	Y	Y	Y	NA	Pixel-wise annotations of OD and OC Localization mask of Fovea Classification labels of normal and glaucomatous	Orlando, J.I.; Fu, H.; Breda, J.B.; van Keer, K.; Bathula, D.R.; Diaz-Pinto, A.; Fang, R.; Heng, P.A.; Kim, J.; Lee, J.; et al. REFUGE Challenge: A unified framework for evaluating automated methods for glaucoma assessment from fundus photographs. Med Image Anal. 2020, 59, 101570. [CrossRef]
RIGA	Retinal images for glaucoma analysis (RIGA)	https://deepblue.lib.umich.edu/data/concern/data_sets/3b591905z	Y	5250	NA	NA	NA	JPEG & TIFF	Y	NA	Y	Y	NA	NA
RIM-ONE	RIM-ONE (v1 ~ v3)	http://medimrg.webs.ull.es/research/retinal-imaging/rim-one/	Y	159	85	74	2144 X 1424	JPEG	Y	NA	NA	Y	Manual segmentation masks of OD Classification labels of normal and glaucomatous	Fumero, F.; Alayón, S.; Sanchez, J.L.; Sigut, J.; Gonzalez-Hernandez, M. RIM-ONE: An open retinal image database for optic nerve evaluation. In Proceedings of the 2011 24th International Symposium on Computer-Based Medical Systems (CBMS), Bristol, UK, 27–30 June 2011; pp. 1–6. [CrossRef]
SCES	SCES	NA	N	1676	1630	46	NA	NA	NA	Y	N	NA	Classification labels of normal and glaucomatous	Pan, C.W.;Wong, T.Y.; Chang, L.; Lin, X.Y.; Lavanya, R.; Zheng, Y.F.; Kok, Y.O.;Wu, R.Y.; Aung, T.; Saw, S.M. Ocular biometry in an urban Indian population: The Singapore Indian Eye Study (SINDI). Investig. Ophthalmol. Vis. Sci. 2011, 52, 6636–6642. [CrossRef]
Shifa	Department of Ophthalmology, Shifa International	NA	N	111	19	92	1936 X 1296	NA	NA	NA	NA	NA	NA	NA

	Hospital property													
STARE	STructured Analysis of the Retina	http://cecas.clemson.edu/~ahoover/stare/	Y	400	NA	NA	NA	NA	Y	Y	Y	Y	NA	NA
ONHSD	Optic nerve head segmentation	NA	N	99	NA	38	760×570	NA	Y	NA	NA	NA	NA	NA

Table3. A comparison between different available retinal image segmentation & localization techniques

Author	Dataset	Public (Y/N)	Method	Performance	Time (s)	Localization	Segmentation
Thangaraj & Natarajan, 2017	RIM-ONE	Y	Classification SVM is used for Glaucoma diagnosis	Accuracy: 93%	NA		Classification
Mohamed et al., 2019	RIM-ONE	Y	An automated glaucoma screening system using cup-to-disc ratio viaSimple Linear Iterative Clustering superpixel	the system achieved 98.6% accu-racy, 97.6% sensitivity and 92.3% specificity for the linear kernelwith the optimal number of the superpixel generated, k = 200	NA	Y	Y
Nugraha & Soesanti, 2016	RIM-ONE	Y	Segmentation of the Optic Disc and Optic Cup Using Histogram Feature-Based Adaptive Threshold for Cup to Disc Ratio	No much details on results		N	Y

Tabassum et al., 2020	RIM-ONE	Y	using Cup Disc Encoder Decoder Network (CDED-Net) for the joint segmentation of optic disc (OD) and optic cup (OC) Segmentation of (OD) and OC is modeled as a semantic pixel-wise labeling problem.	DC(F) // JC(O) // Sensitivity // Specificity
				OD: 95.82 // 91.01 // 97.34 // 99.73
				OC: 86.22 // 75.32 // 95.17 // 99.81
					NA	N	Y

Sreng et al., 2020	RIM-ONE	Y	Deep Learning "ensemble learning" for Optic Disc Segmentation and Glaucoma Diagnosis on Retinal Images (1) transfer learning and (2) learning the feature descriptors using support vector machine and (3) building ensemble of methods in (1) and (2). automatic glaucoma detection system using deep learning has two-stages. In the first stage, DeepLabv3+ detected and extracted the OD from the entire image. In the second stage, three styles of deep CNNs were used to identify between normal and glaucoma in the segmented OD region.	Accuracy: 97.37% AUC: 100%	NA	Y	Y
Xu et al., 2019	RIM-ONE	Y	U-shaped CNN with multi-scale and multi-kernel module (MSMKU) for OD and OC segmentation	F-Score // IoU // Sensitivity // Specificity OD: 0.9561 // 0.9172 // 0.9521 // 0.9987 OC: 0.8564 // 0.7586 // 0.8515 // 0.9971	NA	N	Y
Yu et al., 2019	RIM-ONE	Y	developed a robust segmentation method for optic disc and cup segmentation using a modified U-Net architecture, which combines the widely adopted pre-trained ResNet-34 model as encoding layers with classical U-Net decoding layers. The model was trained on the newly available RIGA dataset, and achieved an average dice value of 97.31% for disc segmentation and 87.61% for cup segmentation, // RIGA (training only + experts results)	Dice Coefficient // Jaccard Coefficient OD : 94.91% // 90.65% OC : 79.32% // 68.28%	NA	Y	Y
Wang et al., 2019	RIM-ONE	Y	patch-based Output Space Adversarial Learning framework (pOSAL) to jointly and robustly segment the OD and OC from different fundus image datasets	Dice Index OD = 0.865, OC = 0.787	NA	Y	Y
Al-Bander et al., 2018	RIM-ONE	Y	"FC-DenseNet" -- Dense Net + Fully CNN "FCN" // ORIGA for training only 1- propose a new strategy of using FC-DenseNet for simultaneous	OD 0.6903 0.5567 OC 0.9036 0.8289 RIM 0.7341 0.5942	NA	N	Y

			semantic segmentation of the cup and disc in fundus images. 2- We determine the optic disc diameter (ODD) and use this to crop the images to 2ODD and rescale. 3- We also demonstrate the effectiveness of this method on other datasets without the need of re-training the model using images from those datasets.				
Shankaranarayana et al., 2017	RIM-ONE	Y	* end to end, fully convolutional, encoder-decoder type network for this task * propose a novel architecture called ResU-net inspired from RESNET, * modified U-net architecture as generator in GAN, * modified U-net architecture as generator in conditional GAN	ResU-net OD F score = 0.977, OD IoU = 0.901, OC F Score = 0.945, OC IoU = 0.786 ResU-GAN OD F Score = 0.987, OD IoU = 0.961, OC F Score = 0.906, OC IoU = 0.739 ResU-cGAN OD F Score = 0.977, OD IoU = 0.897, OC F Score = 0.940, OC IoU = 0.768	NA	N	Y
Sevastopolsky, 2017	RIM-ONE	Y	Modification of U-Net Convolutional Neural Network for Optic Disc and Cup Segmentation Methods for Glaucoma Detection	OD segmentation IoU = 0.89, Dice = 0.95 OC segmentation IoU = 0.69, Dice = 0.82	OD Training = 9932, OD Prediction = 0.1 OC prediction = 0.06	N	Y
Sreng et al., 2020	ORIGA	Y	Deep Learning "ensemble learning" for Optic Disc Segmentation and Glaucoma Diagnosis on Retinal Images (1) transfer learning and (2) learning the feature descriptors using support vector machine and (3) building ensemble of methods in (1) and (2). automatic glaucoma detection system using deep learning has two-stages. In the first stage, DeepLabv3+ detected and extracted the OD from the entire image. In the second stage, three styles of deep CNNs were used to identify between normal and glaucoma in the segmented OD region.	Accuracy: 90% AUC: 92.06%	NA	Y	Y
Jiang et al., 2019	ORIGA	Y	end-to-end region-based convolutional neural network for joint optic disc and cup segmentation (referred to as Joint RCNN)	Overlapping Error // CDR Error OD: 0.063 OC: 0.209 // CDR: 0.068	NA	Y	Y
Jiang et al., 2018	ORIGA	Y	Optic Disc and Cup Segmentation with Blood Vessel Removal from Fundus Images for Glaucoma Detection using Faster RCNN for object detection instead of segmentation to get OD/OC bounding box	Error Disc & Error Cup Faster R-CNN 0.070 0.223 DeepVessel + Faster R-CNN 0.069 0.222	NA	Y	Y
Al-Bander et al., 2018	ORIGA	Y	"FC-DenseNet" -- Dense Net + Fully CNN "FCN" // ORIGA for training only 1- propose a new strategy of using FC-DenseNet for simultaneous semantic segmentation of the cup and disc in fundus images. 2- We determine the optic disc diameter (ODD) and use this to crop the images to 2ODD and rescale. 3- We also demonstrate the effectiveness of this method on other datasets without the need of re-training the model using images from those datasets.	Dice & Jaccard OD 0.8659 0.7688 OC 0.9653 0.9334	NA	N	Y

Fu et al., 2018	ORIGA	Y	Joint OD & OC segmentation using M-NET Deep learning architecture multi label and polar transformation	delta Error Our M-Net 0.078 Joint U-Net + PT 0.074 Our M-Net + PT 0.071 CDR RDAR Our M-Net 0.8019 0.7981 Joint U-Net + PT 0.8152 0.7921 Our M-Net + PT 0.8508 0.8425	NA	Y	Y
P. Xu et al., 2017	ORIGA	Y	OD Localization using CNN and pixel sorting based on threshold	ORIGA Localization Accuracy: 100%	0.93	Y	N

[1] "Glaucoma," WebMD. Accessed: Oct. 04, 2021. [Online]. Available: https://www.webmd.com/eye-health/glaucoma-eyes

[2] "Glaucoma," nhs.uk. Accessed: Oct. 04, 2021. [Online]. Available: https://www.nhs.uk/conditions/glaucoma/

[3] I. en Español, A. Statement, P. Policy, T. & C. of Use, and P. Credits, "Glaucoma Facts and Stats," Glaucoma Research Foundation. Accessed: Oct. 03, 2021. [Online]. Available: https://www.glaucoma.org/glaucoma/glaucoma-facts-and-stats.php

[4] H.-J. Kwon and S.-W. Park, "Fundus Examination," in *Primary Eye Examination: A Comprehensive Guide to Diagnosis*, J.-S. Lee, Ed., Singapore: Springer, 2019, pp. 209–227. doi: 10.1007/978-981-10-6940-6_15.

[5] C. E. Willoughby, D. Ponzin, S. Ferrari, A. Lobo, K. Landau, and Y. Omidi, "Anatomy and physiology of the human eye: effects of mucopolysaccharidoses disease on structure and function – a review," *Clin. Experiment. Ophthalmol.*, vol. 38, no. s1, pp. 2–11, 2010, doi: 10.1111/j.1442-9071.2010.02363.x.

[6] "Optic Nerve," Physiopedia. Accessed: Oct. 06, 2021. [Online]. Available: https://www.physio-pedia.com/Optic_Nerve

[7] "Optic Nerve Anatomy," Verywell Health. Accessed: Oct. 06, 2021. [Online]. Available: https://www.verywellhealth.com/optic-nerve-anatomy-4686150

[8] J. Lowell *et al.*, "Optic Nerve Head Segmentation," *IEEE Trans. Med. Imaging*, vol. 23, no. 2, pp. 256–264, Feb. 2004, doi: 10.1109/TMI.2003.823261.

[9] H. Kolb, "Gross Anatomy of the Eye," in *Webvision: The Organization of the Retina and Visual System*, H. Kolb, E. Fernandez, and R. Nelson, Eds., Salt Lake City (UT): University of Utah Health Sciences Center, 1995. Accessed: Oct. 22, 2021. [Online]. Available: http://www.ncbi.nlm.nih.gov/books/NBK11534/

[10] "Statistics," Glaucoma Information. Accessed: Oct. 25, 2021. [Online]. Available: https://www.glaucomapatients.org/basic/statistics/

[11] A. Issac, M. Parthasarthi, and M. K. Dutta, "An adaptive threshold based algorithm for optic disc and cup segmentation in fundus images," in *2015 2nd International Conference on Signal Processing and Integrated Networks (SPIN)*, Noida, Delhi-NCR, India: IEEE, Feb. 2015, pp. 143–147. doi: 10.1109/SPIN.2015.7095384.

[12] G. S. Nugraha and I. Soesanti, "Segmentation of the Optic Disc and Optic Cup Using Histogram Feature-Based Adaptive Threshold for Cup to Disk Ratio," *MATEC Web Conf.*, vol. 75, p. 05003, 2016, doi: 10.1051/matecconf/20167505003.

[13] A. Singh, M. K. Dutta, M. Parthasarathi, R. Burget, and K. Riha, "An efficient automatic method of Optic disc segmentation using region growing technique in retinal images," in *2014 International Conference on Contemporary Computing and Informatics (IC3I)*, Nov. 2014, pp. 480–484. doi: 10.1109/IC3I.2014.7019713.

[14] S. Omid, J. Shanbehzadeh, Z. Ghassabi, and S. S. Ostadzadeh, "Optic disc detection in high-resolution retinal fundus images by region growing," in *2015 8th International Conference on Biomedical Engineering and Informatics (BMEI)*, Oct. 2015, pp. 101–105. doi: 10.1109/BMEI.2015.7401481.

[15] N. D. Salih, M. D. Saleh, C. Eswaran, and J. Abdullah, "Fast optic disc segmentation using FFT-based template-matching and region-growing techniques," *Comput. Methods Biomech. Biomed. Eng. Imaging Vis.*, vol. 6, no. 1, pp. 101–112, Jan. 2018, doi: 10.1080/21681163.2016.1182071.

[16] F. Yin *et al.*, "Automated segmentation of optic disc and optic cup in fundus images for glaucoma diagnosis," in *2012 25th IEEE International Symposium on Computer-Based Medical Systems (CBMS)*, Jun. 2012, pp. 1–6. doi: 10.1109/CBMS.2012.6266344.

[17] J. Cheng *et al.*, "Superpixel Classification Based Optic Disc and Optic Cup Segmentation for Glaucoma Screening," *IEEE Trans. Med. Imaging*, vol. 32, no. 6, pp. 1019–1032, Jun. 2013, doi: 10.1109/TMI.2013.2247770.

[18] J. Ayub *et al.*, "Glaucoma detection through optic disc and cup segmentation using K-mean clustering," in *2016 International Conference on Computing, Electronic and Electrical Engineering (ICE Cube)*, Apr. 2016, pp. 143–147. doi: 10.1109/ICECUBE.2016.7495212.

[19] N. A. Mohamed, M. A. Zulkifley, W. M. D. W. Zaki, and A. Hussain, "An automated glaucoma screening system using cup-to-disc ratio via Simple Linear Iterative Clustering superpixel approach," *Biomed. Signal Process. Control*, vol. 53, p. 101454, Aug. 2019, doi: 10.1016/j.bspc.2019.01.003.

[20] Z. U. Rehman, S. S. Naqvi, T. M. Khan, M. Arsalan, M. A. Khan, and M. A. Khalil, "Multi-parametric optic disc segmentation using superpixel based feature classification," *Expert Syst. Appl.*, vol. 120, pp. 461–473, Apr. 2019, doi: 10.1016/j.eswa.2018.12.008.

[21] P. V. Rao, R. Gayathri, and R. Sunitha, "A Novel Approach for Design and Analysis of Diabetic Retinopathy Glaucoma Detection Using Cup to Disk Ration and ANN," *Procedia Mater. Sci.*, vol. 10, pp. 446–454, Jan. 2015, doi: 10.1016/j.mspro.2015.06.080.

[22] W. Ruengkitpinyo, P. Vejjanugraha, W. Kongprawechnon, T. Kondo, P. Bunnun, and H. Kaneko, "An automatic glaucoma screening algorithm using cup-to-disc ratio and ISNT rule with support vector machine," in *IECON 2015 - 41st Annual Conference of the IEEE Industrial Electronics Society*, Nov. 2015, pp. 000517–000521. doi: 10.1109/IECON.2015.7392152.

[23] A. Dey and S. K. Bandyopadhyay, "Automated Glaucoma Detection Using Support Vector Machine Classification Method," *J. Adv. Med. Med. Res.*, pp. 1–12, 2016, doi: 10.9734/BJMMR/2016/19617.

[24] J. Cheng, D. Tao, D. W. K. Wong, and J. Liu, "Quadratic divergence regularized SVM for optic disc segmentation," *Biomed. Opt. Express*, vol. 8, no. 5, pp. 2687–2696, May 2017, doi: 10.1364/BOE.8.002687.

[25] V. Thangaraj and V. Natarajan, "Glaucoma diagnosis using support vector machine," in *2017 International Conference on Intelligent Computing and Control Systems (ICICCS)*, Jun. 2017, pp. 394–399. doi: 10.1109/ICCONS.2017.8250750.

[26] M. Abdullah, M. M. Fraz, and S. A. Barman, "Localization and segmentation of optic disc in retinal images using circular Hough transform and grow-cut algorithm," *PeerJ*, vol. 4, p. e2003, 2016, doi: 10.7717/peerj.2003.

[27] S. Sedai, P. K. Roy, D. Mahapatra, and R. Garnavi, "Segmentation of optic disc and optic cup in retinal fundus images using shape regression," *Annu. Int. Conf. IEEE Eng. Med. Biol. Soc. IEEE Eng. Med. Biol. Soc. Annu. Int. Conf.*, vol. 2016, pp. 3260–3264, Aug. 2016, doi: 10.1109/EMBC.2016.7591424.

[28] A. Sevastopolsky, "Optic disc and cup segmentation methods for glaucoma detection with modification of U-Net convolutional neural network," *Pattern Recognit. Image Anal.*, vol. 27, no. 3, pp. 618–624, 2017.

[29] S. M. Shankaranarayana, K. Ram, K. Mitra, and M. Sivaprakasam, "Joint Optic Disc and Cup Segmentation Using Fully Convolutional and Adversarial Networks," in *Fetal, Infant and Ophthalmic Medical Image Analysis*, M. J. Cardoso, T. Arbel, A. Melbourne, H. Bogunovic, P.

Moeskops, X. Chen, E. Schwartz, M. Garvin, E. Robinson, E. Trucco, M. Ebner, Y. Xu, A. Makropoulos, A. Desjardin, and T. Vercauteren, Eds., in Lecture Notes in Computer Science. Cham: Springer International Publishing, 2017, pp. 168–176. doi: 10.1007/978-3-319-67561-9_19.

[30] P. Xu, C. Wan, J. Cheng, D. Niu, and J. Liu, "Optic Disc Detection via Deep Learning in Fundus Images," in *Fetal, Infant and Ophthalmic Medical Image Analysis*, M. J. Cardoso, T. Arbel, A. Melbourne, H. Bogunovic, P. Moeskops, X. Chen, E. Schwartz, M. Garvin, E. Robinson, E. Trucco, M. Ebner, Y. Xu, A. Makropoulos, A. Desjardin, and T. Vercauteren, Eds., in Lecture Notes in Computer Science. Cham: Springer International Publishing, 2017, pp. 134–141. doi: 10.1007/978-3-319-67561-9_15.

[31] H. Fu, J. Cheng, Y. Xu, D. W. K. Wong, J. Liu, and X. Cao, "Joint optic disc and cup segmentation based on multi-label deep network and polar transformation," *IEEE Trans. Med. Imaging*, vol. 37, no. 7, pp. 1597–1605, 2018.

[32] B. Al-Bander, B. M. Williams, W. Al-Nuaimy, M. A. Al-Taee, H. Pratt, and Y. Zheng, "Dense fully convolutional segmentation of the optic disc and cup in colour fundus for glaucoma diagnosis," *Symmetry*, vol. 10, no. 4, p. 87, 2018.

[33] Y. Jiang *et al.*, "Optic Disc and Cup Segmentation with Blood Vessel Removal from Fundus Images for Glaucoma Detection," *Annu. Int. Conf. IEEE Eng. Med. Biol. Soc. IEEE Eng. Med. Biol. Soc. Annu. Int. Conf.*, vol. 2018, pp. 862–865, Jul. 2018, doi: 10.1109/EMBC.2018.8512400.

[34] S. Wang, L. Yu, X. Yang, C.-W. Fu, and P.-A. Heng, "Patch-based output space adversarial learning for joint optic disc and cup segmentation," *IEEE Trans. Med. Imaging*, vol. 38, no. 11, pp. 2485–2495, 2019.

[35] S. Yu, D. Xiao, S. Frost, and Y. Kanagasingam, "Robust optic disc and cup segmentation with deep learning for glaucoma detection," *Comput. Med. Imaging Graph.*, vol. 74, pp. 61–71, 2019.

[36] Y. Jiang *et al.*, "Jointrcnn: A region-based convolutional neural network for optic disc and cup segmentation," *IEEE Trans. Biomed. Eng.*, vol. 67, no. 2, pp. 335–343, 2019.

[37] Y.-L. Xu, S. Lu, H.-X. Li, and R.-R. Li, "Mixed Maximum Loss Design for Optic Disc and Optic Cup Segmentation with Deep Learning from Imbalanced Samples," *Sensors*, vol. 19, no. 20, Oct. 2019, doi: 10.3390/s19204401.

[38] S. Sreng, N. Maneerat, K. Hamamoto, and K. Y. Win, "Deep Learning for Optic Disc Segmentation and Glaucoma Diagnosis on Retinal Images," *Appl. Sci.*, vol. 10, no. 14, Art. no. 14, Jan. 2020, doi: 10.3390/app10144916.

[39] J. Gao, Y. Jiang, H. Zhang, and F. Wang, "Joint disc and cup segmentation based on recurrent fully convolutional network," *PloS One*, vol. 15, no. 9, p. e0238983, 2020.

[40] M. Tabassum *et al.*, "CDED-Net: Joint Segmentation of Optic Disc and Optic Cup for Glaucoma Screening," *IEEE Access*, vol. 8, pp. 102733–102747, 2020, doi: 10.1109/ACCESS.2020.2998635.